

Influence of sol counter-ions on the anatase-to-rutile phase transformation and microstructure of nanocrystalline TiO₂

D.M. Tobaldi,^{a*} R.C. Pullar,^a A.F. Gualtieri,^b A. Belen Jorge,^c R. Binions,^d M.P. Seabra^a and J.A. Labrincha^a

^a *Department of Materials and Ceramic Engineering / CICECO, University of Aveiro, Campus Universitário de Santiago, 3810-193 Aveiro, Portugal.*

^b *Dipartimento di Scienze Chimiche e Geologiche, Università degli studi di Modena e Reggio Emilia, I-41121 Modena, Italy*

^c *Christopher Ingold Building, Department of Chemistry, University College of London, 20 Gordon Street, London, WC1H 0AJ, UK.*

^d *School of Engineering and Materials Science, Queen Mary University of London, London E1 4NS, UK.*

* Corresponding author. Tel.: +351 234 370 041

E-mail addresses: david.tobaldi@ua.pt; david@davidtobaldi.org

Fig. S1 – Graphic output of the Rietveld refinement of the sample **HCL 450/4h**. The black open squares represent the observed pattern, the red line represent the calculated pattern, and the difference curve between observed and calculated profiles is plotted below. The position of reflections is indicated by the small vertical bars (black: anatase; red: rutile, orange brookite, and green: the internal standard used, NIST 676a).

Fig. S2 –XRPD patterns of the samples after being thermally treated at the 800 °C isotherm. a) **HNO₃**; b) **HCl**; c) **HBr** as sources of counter-ions. The vertical bars represent the XRPD peaks of rutile (red, JCPDS-PDF card no. 21-1276).

Fig. S3 – WPPM graphical output of sample **HNO₃ 600/4h**. The black open squares represent the observed pattern, the red line represent the calculated pattern, and the difference curve between observed and calculated profiles is plotted below. The line-brake on the y-axis is supposed to emphasise the goodness of the fitting.

Fig. S4 – Size distribution, as obtained from the WPPM modelling, of sample **HNO₃ 600** at the different dwell time used. a) anatase; b) rutile. The inset shows a magnification in order to highlight the minimum crystalline domain diameter detected.

Fig. S5 – Size distribution, as obtained from the WPPM modelling, of sample **HCl 600** at the different dwell time used. a) anatase; b) rutile. The inset shows a magnification in order to highlight the minimum crystalline domain diameter detected.

Fig. S6 – Size distribution, as obtained from the WPPM modelling, of sample **HBr 600** at the different dwell time used. a) anatase; b) rutile. The inset shows a magnification in order to highlight the minimum crystalline domain diameter detected.

Fig. S7 – Rutile size distribution at the different dwell time used, as obtained from the WPPM modelling, of samples: a) **HNO₃ 800**; b) **HCl 800**; c) **HBr 800**.

Fig. S1

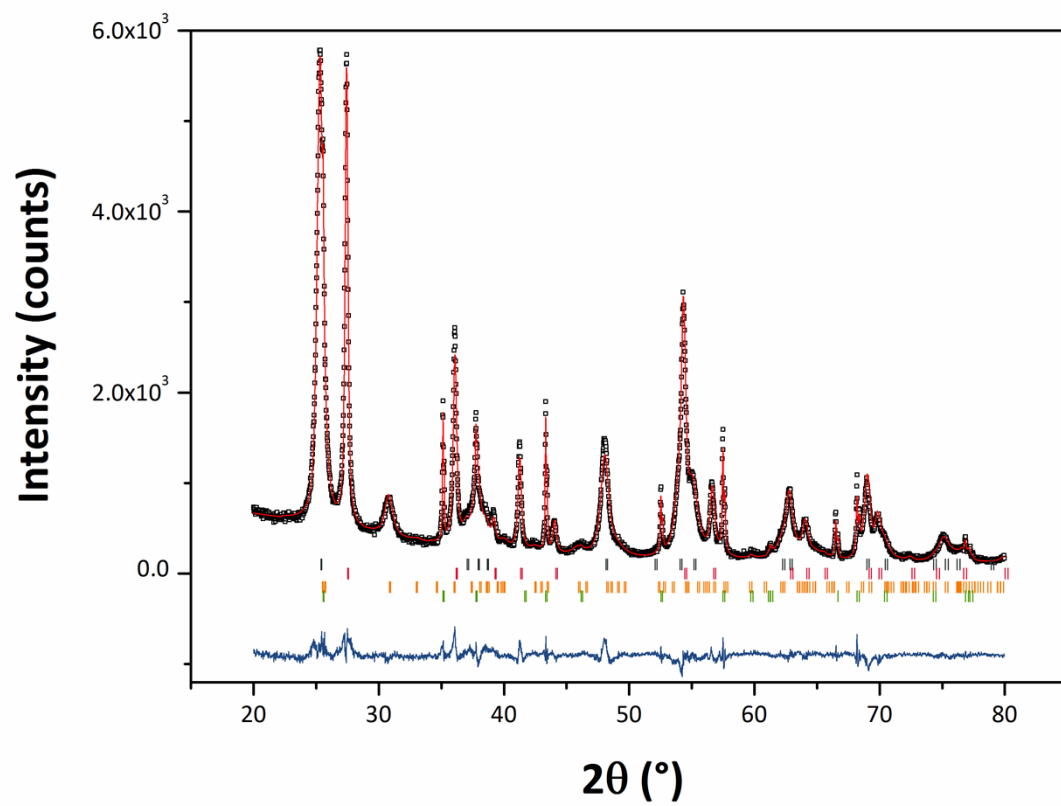


Fig. S2a

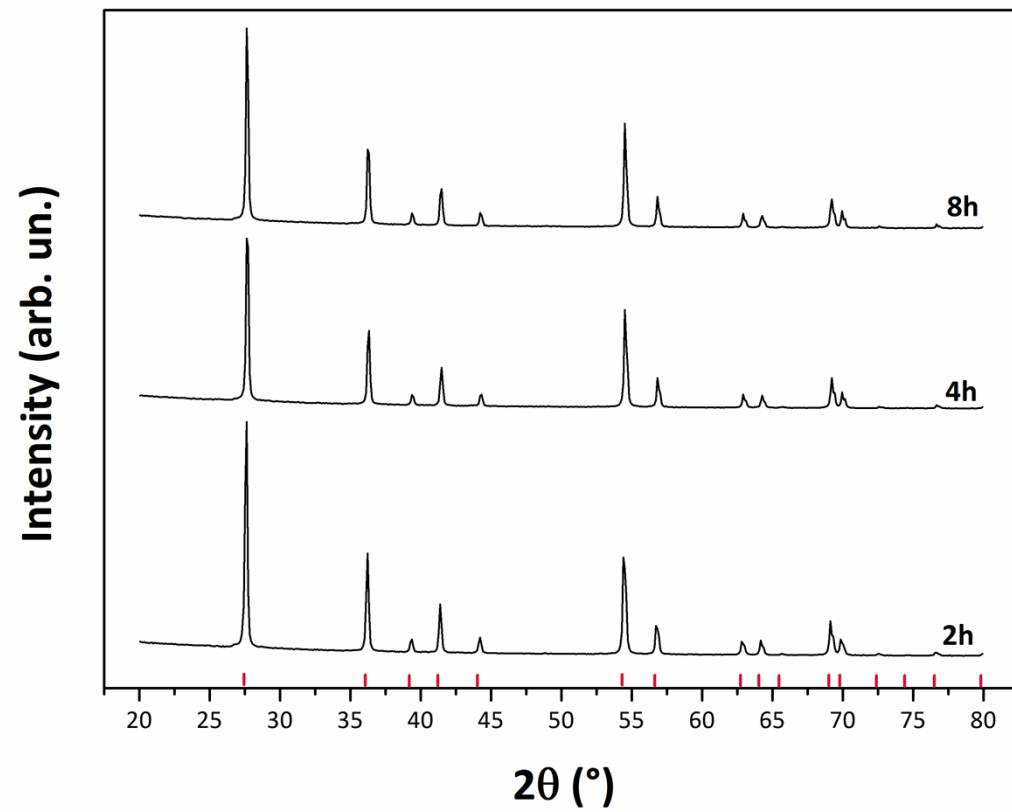


Fig. S2b

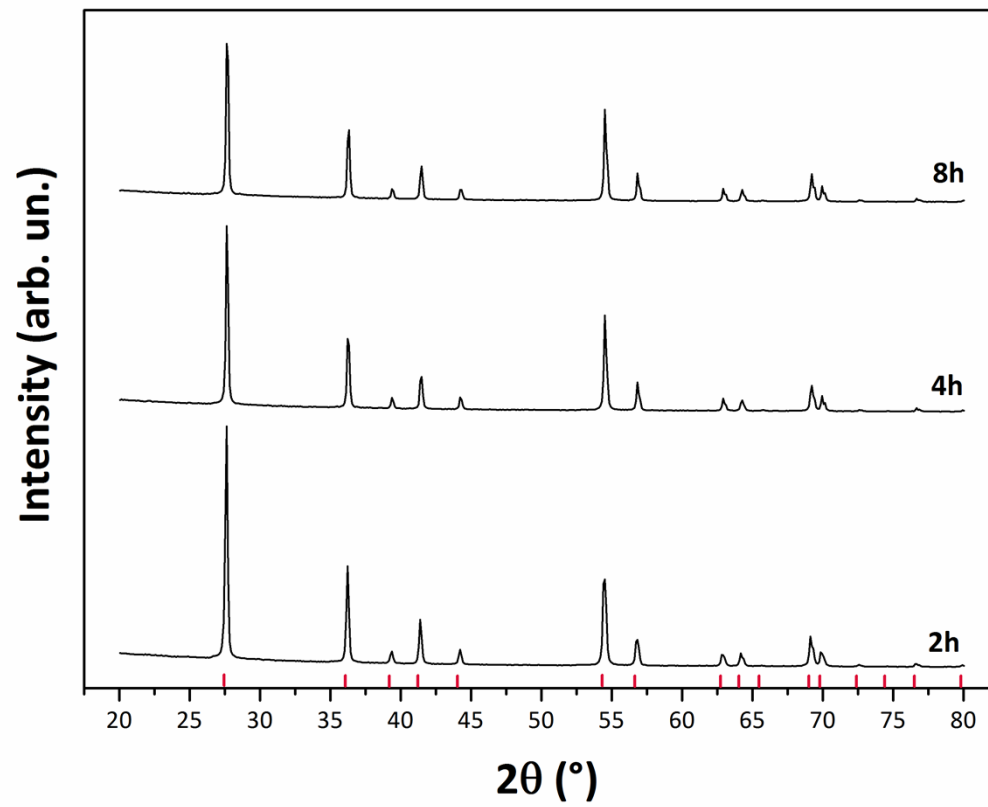


Fig. S2c

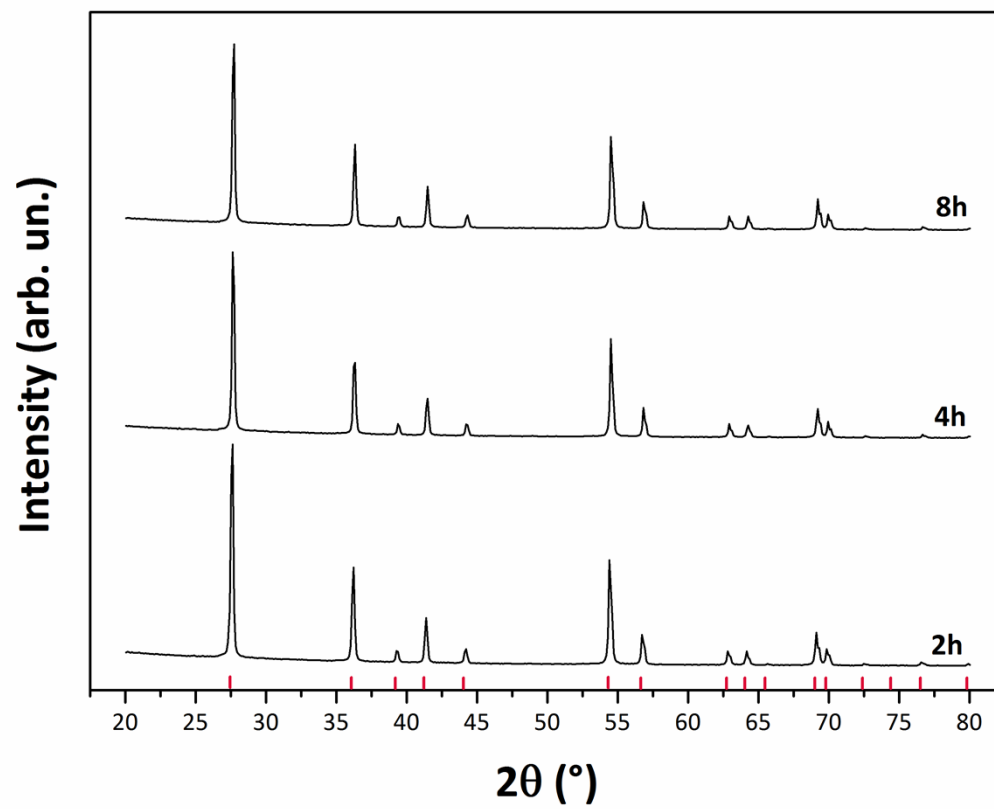


Fig. S3

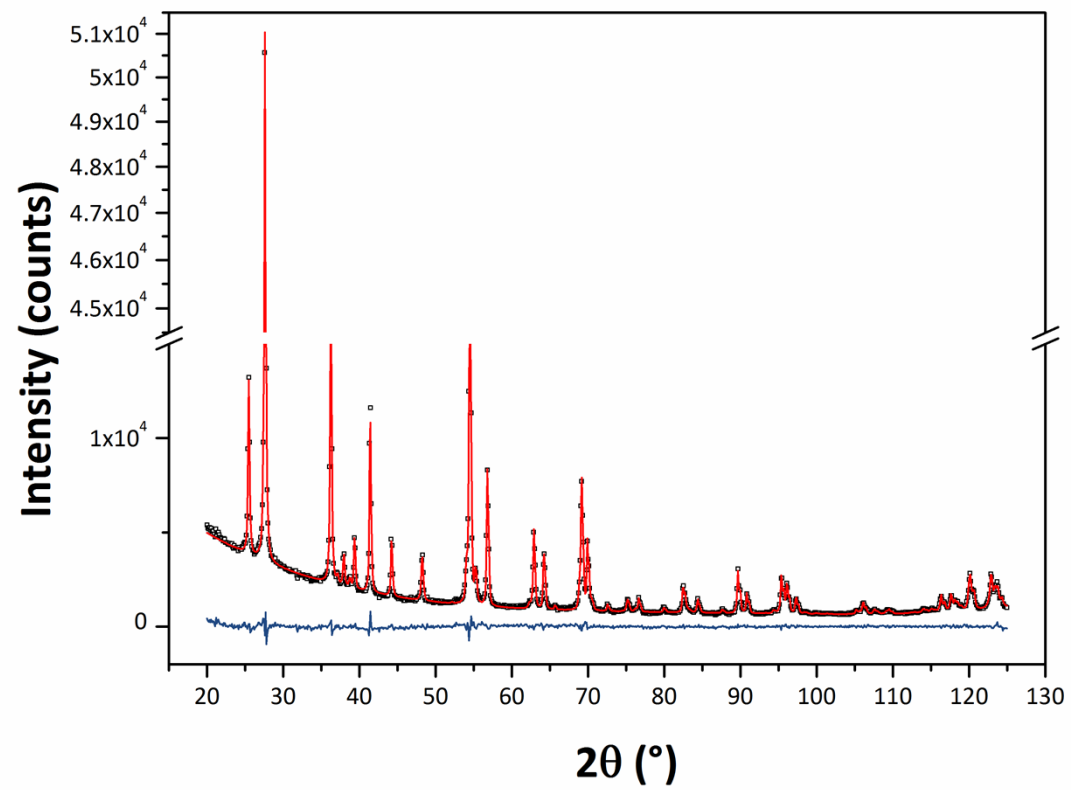


Fig. S4a

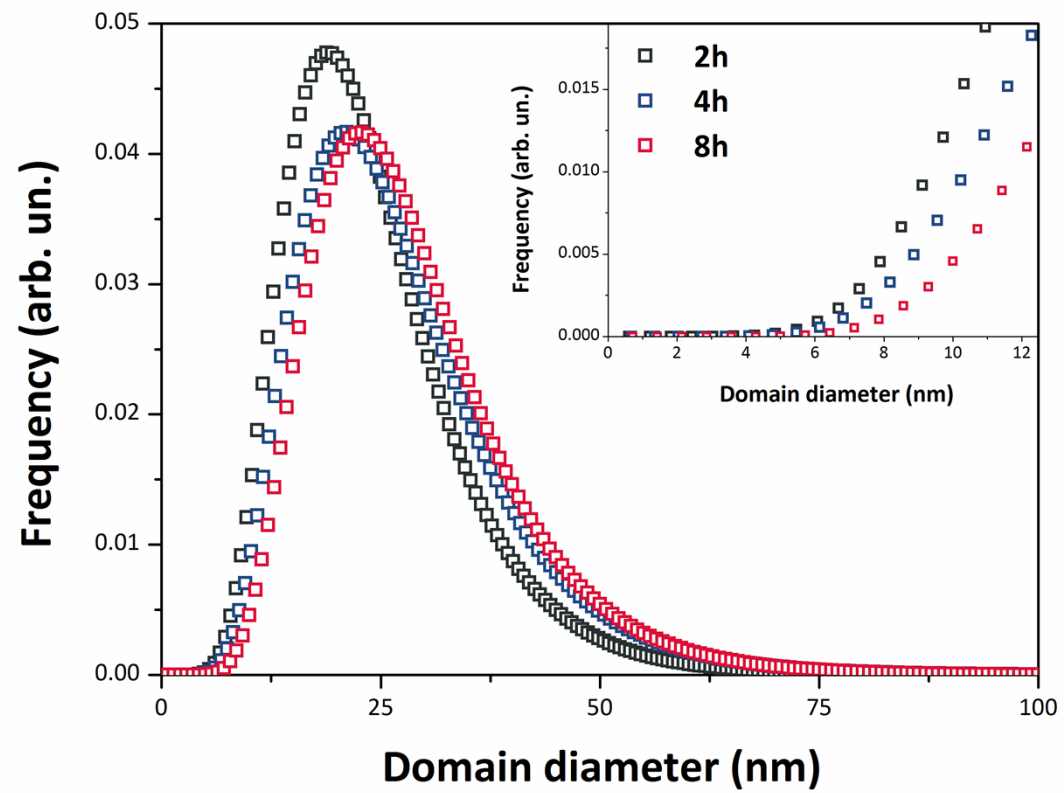


Fig. S4b

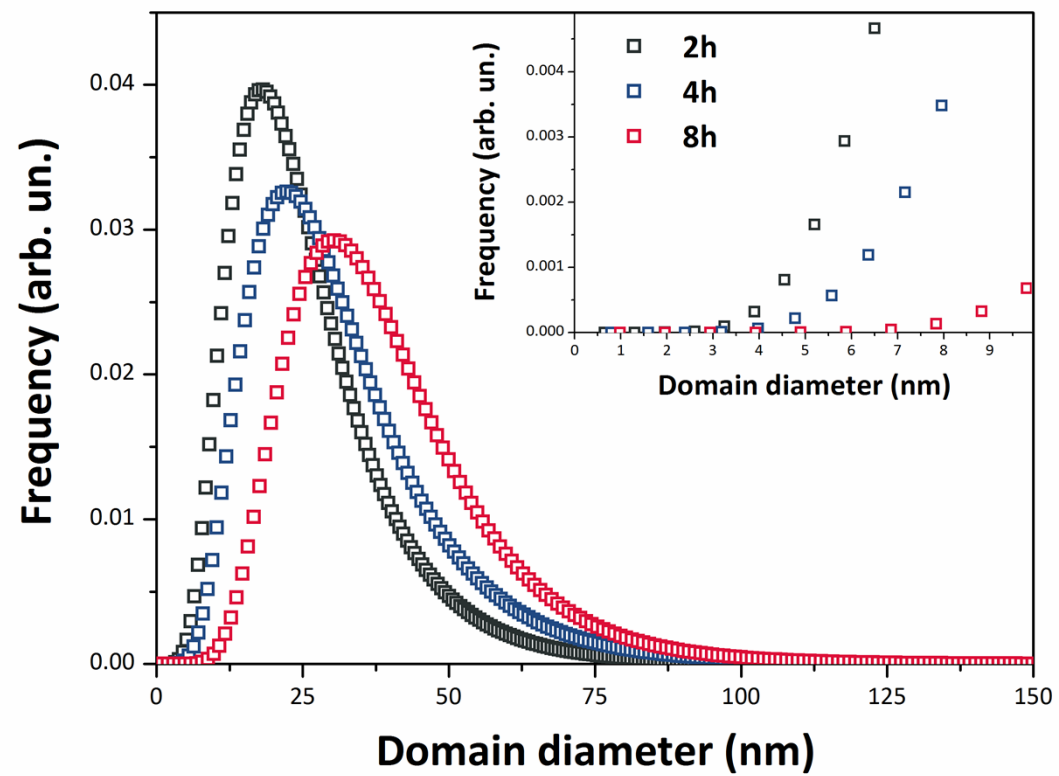


Fig. S5a

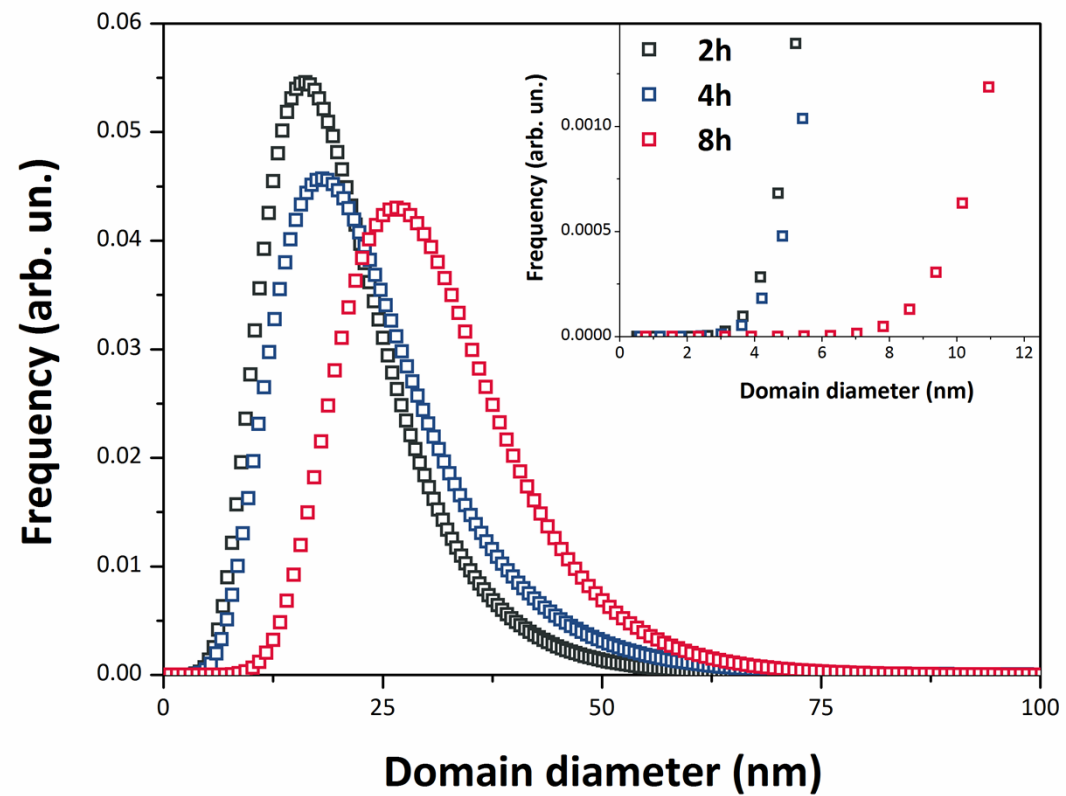


Fig. S5b

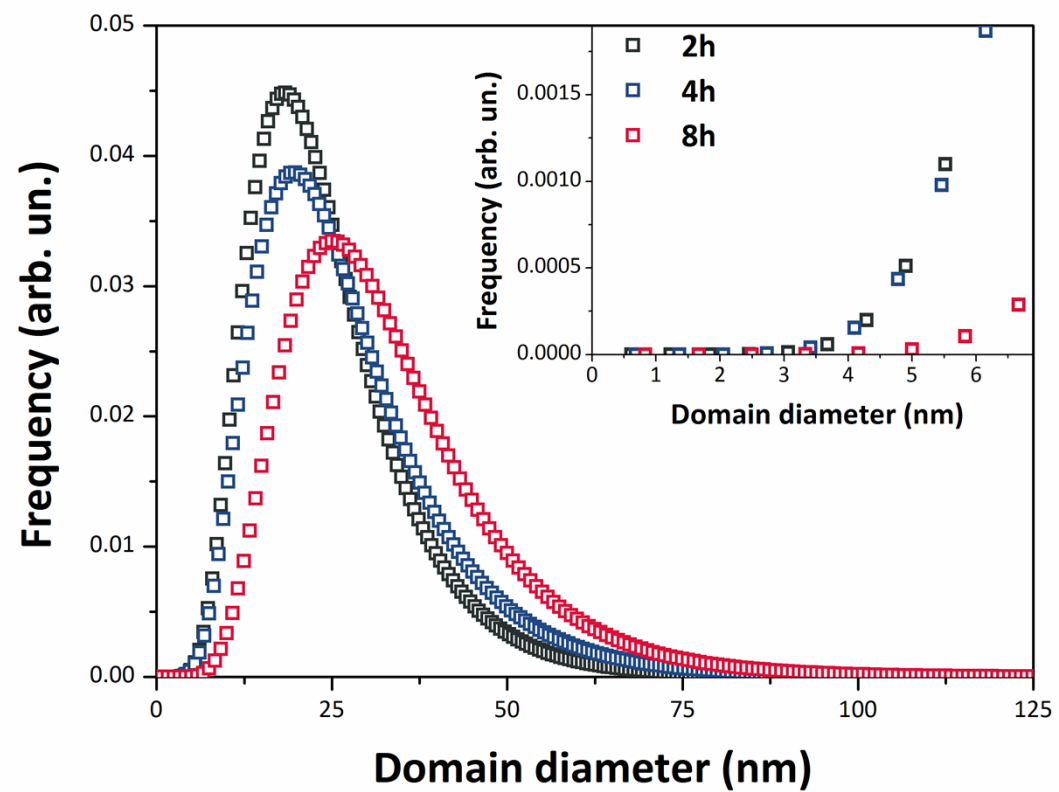


Fig. S6a

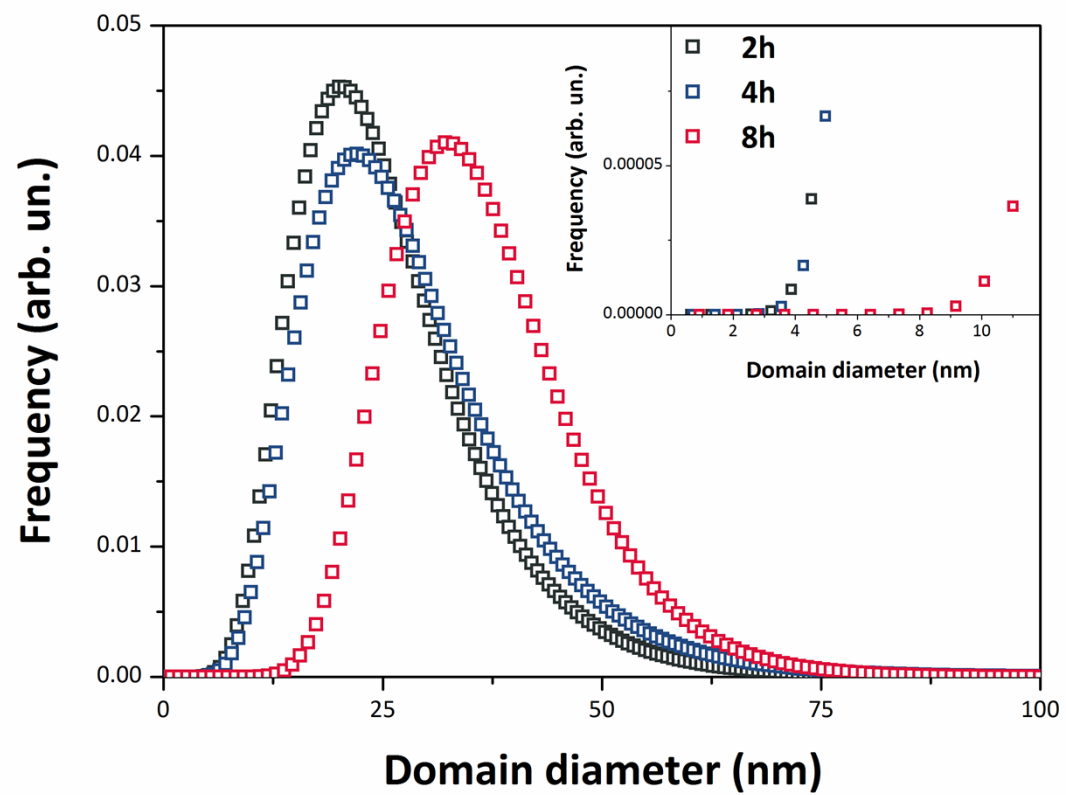


Fig. S6b

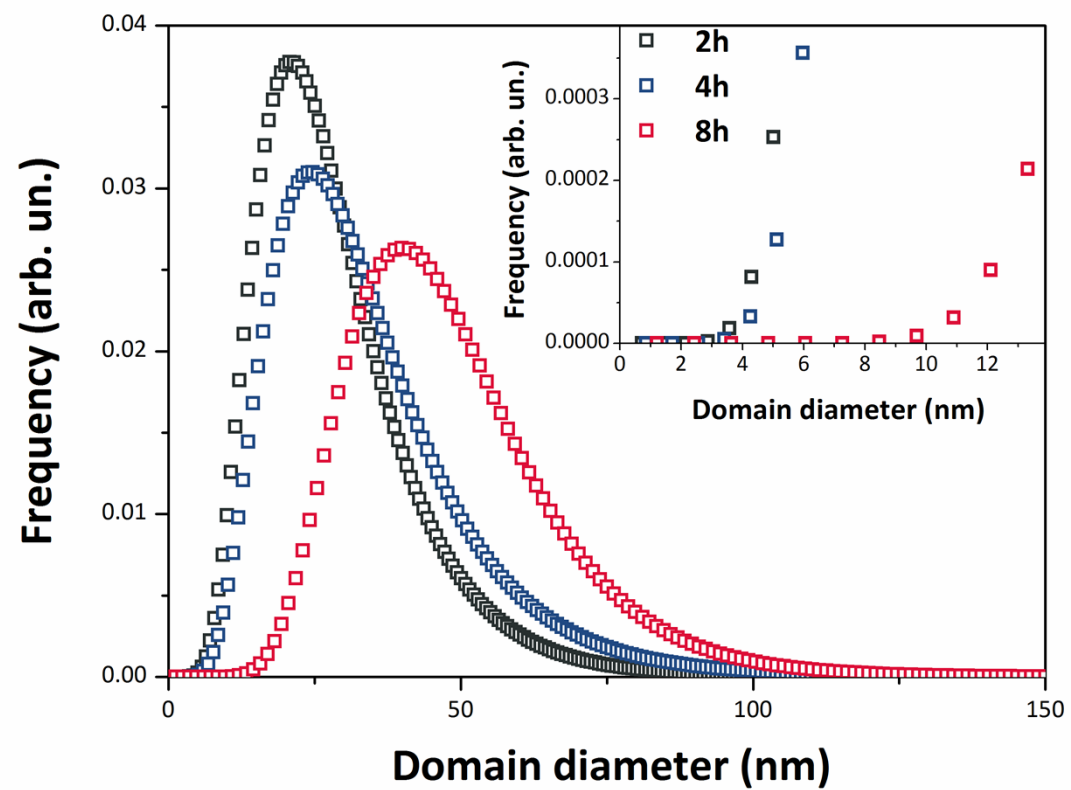


Fig. S7a

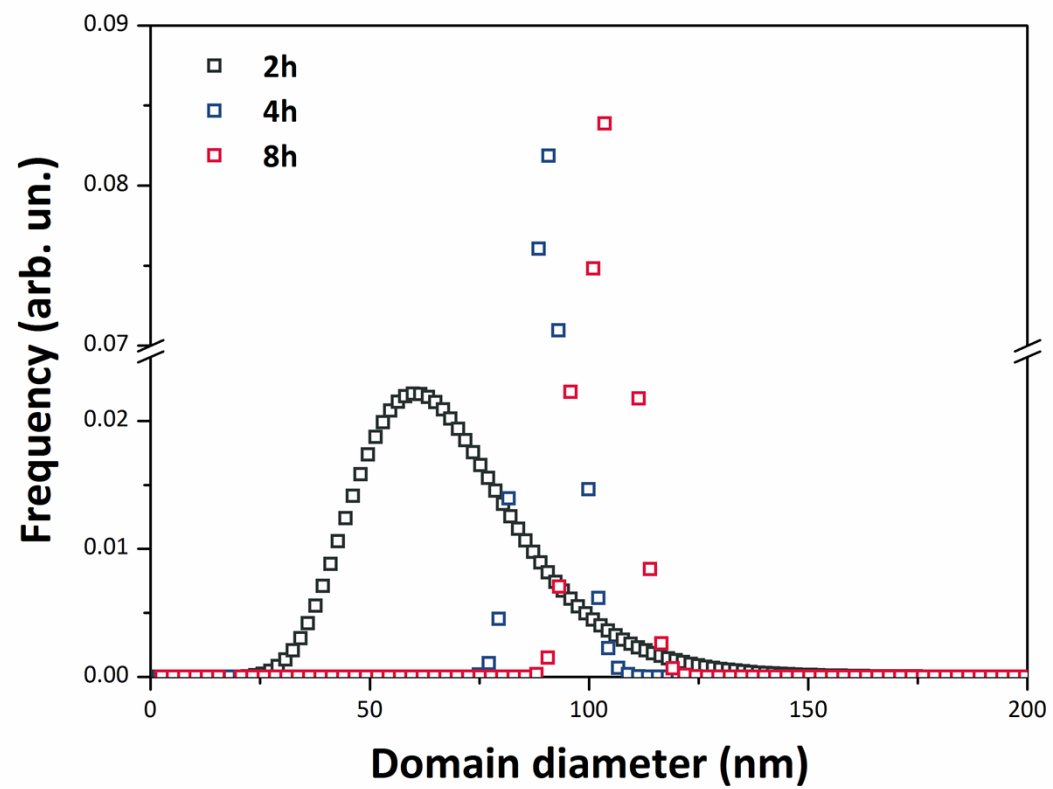


Fig. S7b

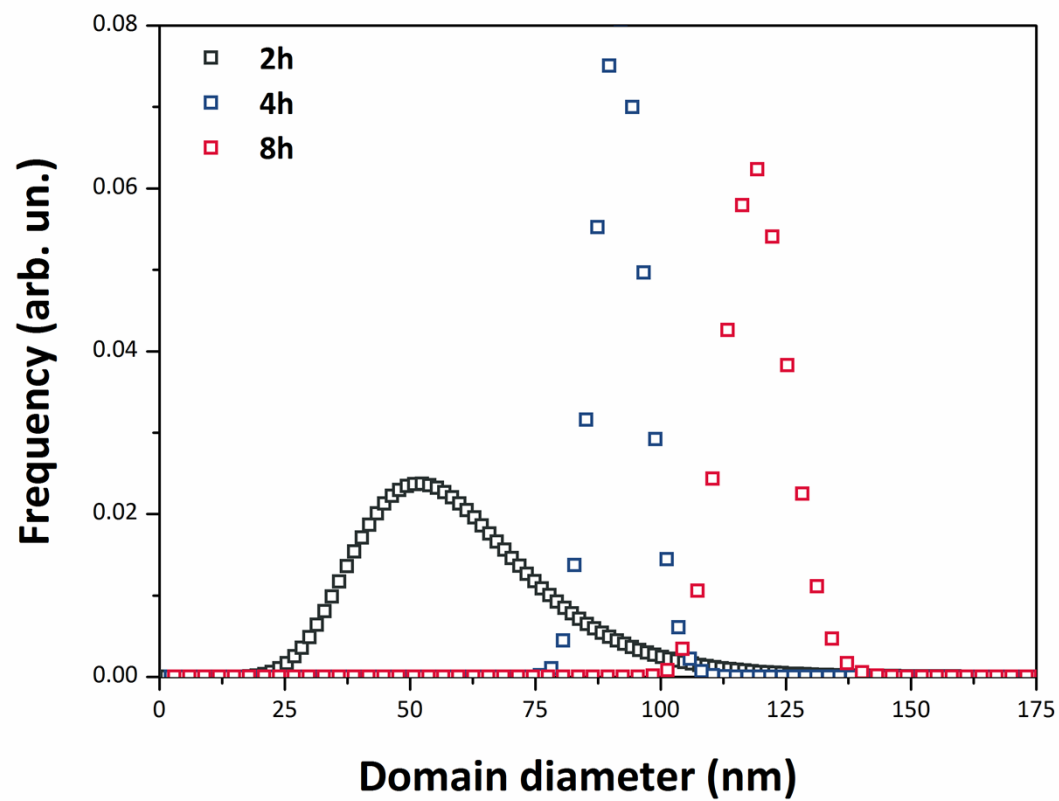


Fig. S7c

